

Results are given of a theoretical and experimental study of the effect of heating the walls of a semiopen tube under conditions of acoustic resonance.

It is well known that acoustic oscillations of a gas column generate nonuniform heating of the tube walls. For large-amplitude resonance oscillations the closed end of the tube may be heated up to 1000°K [1]. The difficulty in a theoretical study of this effect consists primarily in the nonexistence of an acoustic theory of resonance oscillations. In the present paper it is attempted to describe the thermoacoustic effect in a semiopen tube on the basis of an acoustic approximation to the theory of resonance oscillations, obtained for the case of high-frequency oscillations with the use of a nonlinear boundary condition.

Consider gas oscillations in a cylindrical tube of length L and radius R , one of whose edges is a harmonically oscillating piston, the other end of the tube being open. We introduce cylindrical coordinates, so that the piston is located at $x = 0$, the open end is at $x = L$, at the tube axis $r = 0$, and on the wall $r = R$.

The motion and heat exchange of an ideal gas with constant specific heats c_p , c_v , constant coefficients of dynamic viscosity μ and heat conduction λ are described by the equations of motion, continuity, energy, and state. In cylindrical coordinates with axial symmetry they are [1]:

$$\rho \left[\frac{\partial u}{\partial t} + u \frac{\partial u}{\partial x} + v \frac{\partial u}{\partial r} \right] = - \frac{\partial p}{\partial x} + \frac{\mu}{3r} \frac{\partial}{\partial r} \left(r \frac{\partial v}{\partial r} \right) + \frac{4}{3} \mu \frac{\partial^2 u}{\partial x^2} + \frac{\mu}{r} \frac{\partial}{\partial r} \left(r \frac{\partial u}{\partial r} \right), \quad (1a)$$

$$\rho \left[\frac{\partial v}{\partial t} + u \frac{\partial v}{\partial x} + v \frac{\partial v}{\partial r} \right] = - \frac{\partial p}{\partial r} + \frac{4}{3} \mu \left[\frac{1}{r} \frac{\partial}{\partial r} \left(r \frac{\partial v}{\partial r} \right) - \frac{v}{r^2} \right] + \frac{\mu}{3} \frac{\partial^2 v}{\partial x \partial r} + \mu \frac{\partial^2 v}{\partial x^2}, \quad (1b)$$

$$\frac{\partial \rho}{\partial t} + u \frac{\partial \rho}{\partial x} + v \frac{\partial \rho}{\partial r} + \rho \left[\frac{1}{r} \frac{\partial}{\partial r} (vr) + \frac{\partial u}{\partial x} \right] = 0, \quad (1c)$$

$$\begin{aligned} \rho c_p \left[\frac{\partial T}{\partial t} + u \frac{\partial T}{\partial x} + v \frac{\partial T}{\partial r} \right] &= \frac{\partial p}{\partial t} + v \frac{\partial p}{\partial r} + u \frac{\partial p}{\partial x} + \frac{\lambda}{r} \frac{\partial}{\partial r} \left(r \frac{\partial T}{\partial r} \right) + \\ &+ \lambda \frac{\partial^2 T}{\partial x^2} + \frac{4}{3} \mu \left[\left(\frac{\partial v}{\partial r} \right)^2 + \left(\frac{\partial u}{\partial x} \right)^2 + \left(\frac{v}{r} \right)^2 - \frac{v}{r} \frac{\partial v}{\partial r} - \frac{\partial v}{\partial r} \frac{\partial u}{\partial x} - \right. \\ &\left. - \frac{v}{r} \frac{\partial u}{\partial x} \right] + 2\mu \frac{\partial v}{\partial x} \frac{\partial u}{\partial r} + \mu \left(\frac{\partial v}{\partial x} \right)^2 + \mu \left(\frac{\partial u}{\partial r} \right)^2, \end{aligned} \quad (1d)$$

$$p = \rho R_g T. \quad (1e)$$

We assume that oscillations of comparatively weak nonlinearity are established in the tube, i.e., if the parameter $\epsilon = U_\infty/\omega L$ is introduced, it can be assumed to be a small quantity. For a semiopen tube $\epsilon = 0.1$ corresponds to $U_\infty \approx 54$ m/sec.

The assumption of a small ϵ makes it possible to solve the system of equations (1) by a perturbation method, with the solutions sought in the form of a power series expansion in the small parameter ϵ [2].

The general solution of the first approximation equations for a long tube ($R/L \ll 1$) with $T_0 = \text{const}$ was given in [1]. However, the expression for v_1 in [1] does not satisfy the boundary condition on the wall, where both v_1 and u_1 must vanish. Requiring a finite $(v_1)_r$ on the tube axis and $v_1 = 0$ on the wall, we obtain

$$p_1 = \left\{ -A \exp \left[\frac{\omega x}{c_0} \left(\frac{J_0(\psi)}{J_2(\psi)} \frac{\kappa}{n} \right)^{1/2} \right] - B \exp \left[-\frac{\omega x}{c_0} \left(\frac{J_0(\psi)}{J_2(\psi)} \frac{\kappa}{n} \right)^{1/2} \right] \right\} \exp(i\omega t), \quad (2a)$$

$$u_1 = -\frac{i}{\rho_0 c_0} \left(\frac{J_0(\psi)}{J_2(\psi)} \frac{\kappa}{n} \right)^{1/2} \left\{ A \exp \left(\frac{\omega x}{c_0} \left(\frac{J_0(\psi)}{J_2(\psi)} \frac{\kappa}{n} \right)^{1/2} \right) - B \exp \left[-\frac{\omega x}{c_0} \left(\frac{J_0(\psi)}{J_2(\psi)} \frac{\kappa}{n} \right)^{1/2} \right] \right\} \left[1 - \frac{J_0(\psi r/R)}{J_0(\psi)} \right] \exp(i\omega t), \quad (2b)$$

$$v_{1r} = -\frac{i\omega}{\rho_0 c_0^2} \left\{ \frac{(r^2 - R^2)}{2} \left[1 + \frac{J_0(\psi)}{J_2(\psi)} \frac{\kappa}{n} \right] + \frac{(\kappa - 1)R}{\psi \text{Pr}^{1/2}} \frac{[rJ_1(\psi r \text{Pr}^{1/2}/R) - RJ_1(\psi \text{Pr}^{1/2})]}{J_0(\psi \text{Pr}^{1/2})} - \frac{\kappa}{n} \frac{R}{\psi} \frac{[rJ_1(\psi r/R) - RJ_1(\psi)]}{J_2(\psi)} \right\} p_1, \quad (2c)$$

$$\rho_1 = \frac{1}{c_0^2} \left[1 + (\kappa - 1) \frac{J_0(\psi r \text{Pr}^{1/2}/R)}{J_0(\psi \text{Pr}^{1/2})} \right] p_1, \quad (2d)$$

$$T_1 = \frac{1}{\rho_0 c_p} \left[1 - \frac{J_0(\psi r \text{Pr}^{1/2}/R)}{J_0(\psi \text{Pr}^{1/2})} \right] p_1, \quad (2e)$$

where

$$\psi \equiv R \left(\frac{\omega}{v} \right)^{1/2} \exp \left(\frac{3}{4} \pi i \right); \quad \frac{n}{\kappa} = \left[\kappa - (\kappa - 1) \frac{J_2(\psi \text{Pr}^{1/2})}{J_0(\psi \text{Pr}^{1/2})} \right]^{-1}, \quad (3)$$

and the subscript 1 corresponds to the first approximation. We restrict ourselves to the case of high-frequency oscillations, i.e., $R\sqrt{\omega/2\nu} \gg 1$. For air $\text{Pr} = 0.71$, and, consequently, $R\sqrt{\text{Pr}\omega/2\nu} \gg 1$. Using asymptotic expansions of Bessel functions for large argument [3], and performing the replacements

$$A = -\frac{C}{2} \exp(i\alpha), \quad B = -\frac{C}{2} \exp(-i\alpha), \quad (4)$$

expressions (2) can be simplified:

$$p_1 = C \cos(kx + \alpha) \exp(i\omega t), \quad (5)$$

$$u_1 = -\frac{iC}{\rho_0 c_0} \sin(kx + \alpha) \left[1 - \sqrt{\frac{R}{r}} \exp(-(1+i)\sqrt{\omega/2\nu}(R-r)) \right] \exp(i\omega t), \quad (6)$$

$$v_1 = \frac{(i+1)\omega}{2\rho_0 c_0^2} \sqrt{\frac{2\nu}{\omega}} \left\{ \left(\frac{\kappa-1}{\text{Pr}} + 1 \right) \frac{R}{r} - \sqrt{\frac{R}{r}} \left[\exp(-(1+i)\sqrt{\omega/2\nu}(R-r)) \times \sqrt{\omega \text{Pr}/2\nu}(R-r) + \frac{\kappa-1}{\text{Pr}} \exp(-(1+i)\sqrt{\omega/2\nu}(R-r)) \right] \right\} p_1, \quad (7)$$

$$\rho_1 = \frac{1}{c_0^2} \left[1 + (\kappa-1) \sqrt{\frac{R}{r}} \exp(-(1+i)\sqrt{\omega \text{Pr}/2\nu}(R-r)) \right] p_1, \quad (8)$$

$$T_1 = \frac{1}{\rho_0 c_p} \left[1 - \sqrt{\frac{R}{r}} \exp(-(1+i)\sqrt{\omega \text{Pr}/2\nu}(R-r)) \right] p_1. \quad (9)$$

The boundary condition at the piston is [1]

$$u_1(x=0, r=0) = \omega l \exp(i\omega t). \quad (10)$$

Following [4], at the open end we impose the nonlinear condition

$$\left[Z = \frac{p_1(x=L)}{u_1(x=L, r=0)} = Z_u + \frac{1}{2} \rho_0 |u_1(x=L, r=0)|, \right. \\ \left. Z_u = X + iY, \right] \quad (11)$$

where X and Y are determined by the Gutin relations [5]:

$$X = \frac{\rho_0 \omega^2 d^2}{16c_0}, \quad Y = \frac{\rho_0 \omega d}{\pi}. \quad (12)$$

Putting $C = |C|(\cos \varphi + i \sin \varphi)$, $\alpha = \alpha_0 + i\beta$, the boundary conditions (10), (11) give in the near-resonance region the following system for determining $|C|$, φ , α_0 , and β after some transformations:

$$\begin{aligned} \alpha_0 &= \operatorname{ctg} kL - \bar{Y}, \quad \beta = \bar{X} + \frac{1}{2} |\bar{C}| \sin kL, \quad \operatorname{tg} \varphi = \alpha_0/\beta, \\ M &= |\bar{C}| \sqrt{(\operatorname{ctg} kL - \bar{Y})^2 + \left(\bar{X} + \frac{1}{2} |\bar{C}| \sin kL\right)^2}, \end{aligned} \quad (13)$$

where $M = \omega l/c_0$; $\bar{Y} = Y/\rho_0 c_0$; $\bar{X} = X/\rho_0 c_0$; $|\bar{C}| = |C|/\rho_0 c_0^2$.

Expressions (5) and (6) can be reduced to the form

$$p_1 = \rho_0 c_0^2 |\bar{C}| [\cos(kx + \alpha_0) \operatorname{ch} \beta + i \sin(kx + \alpha_0) \operatorname{sh} \beta] \exp(i\omega t), \quad (14)$$

$$u_1 = c_0 |\bar{C}| [\cos(kx + \alpha_0) \operatorname{sh} \beta - i \sin(kx + \alpha_0) \operatorname{ch} \beta] \exp(i\omega t) \left[1 - \sqrt{\frac{R}{r}} \exp(-(1+i)V\omega/2v(R-r)) \right]. \quad (15)$$

The heating effect of tube walls is determined by the terms having a nonvanishing averaged part. Therefore, only even-ordered terms provide a contribution:

$$\langle q \rangle = -\lambda \left\langle \frac{\partial T_2}{\partial r} \Big|_{r=R} + \frac{\partial T_4}{\partial r} \Big|_{r=R} + \dots \right\rangle. \quad (16)$$

The second-order equations with boundary conditions are

$$\begin{aligned} \frac{\partial p_2}{\partial r} &= 0, \\ \rho_0 \frac{\partial u_2}{\partial t} + \frac{\partial p_2}{\partial x} - \mu \frac{1}{r} \frac{\partial}{\partial r} \left(r \frac{\partial u_2}{\partial r} \right) &= -\rho_0 \left(u_1 \frac{\partial u_1}{\partial x} + v_1 \frac{\partial u_1}{\partial r} \right) - \rho_1 \frac{\partial u_1}{\partial t} \\ \frac{\partial p_2}{\partial t} + \rho_0 \left[\frac{\partial v_2}{\partial r} + \frac{v_2}{r} + \frac{\partial u_2}{\partial x} \right] &= -v_1 \frac{\partial p_1}{\partial r} - u_1 \frac{\partial p_1}{\partial x} - \rho_1 \left[\frac{\partial v_1}{\partial r} + \frac{v_1}{r} + \frac{\partial u_1}{\partial x} \right], \\ \rho_0 c_p \frac{\partial T_2}{\partial t} - \frac{\partial p_2}{\partial t} - \frac{\lambda}{r} \frac{\partial}{\partial r} \left(r \frac{\partial T_2}{\partial r} \right) &= -\rho_0 c_p \left[u_1 \frac{\partial T_1}{\partial x} + v_1 \frac{\partial T_1}{\partial r} \right] - \rho_1 c_p \frac{\partial T_1}{\partial t} + \mu \left(\frac{\partial u_1}{\partial r} \right)^2 + u_1 \frac{\partial p_1}{\partial x}, \\ p_2 - \rho_0 R_g T_2 - \rho_2 R_g T_0 &= \rho_1 R_g T_1; \quad u_2 = v_2 = T_2 = 0, \quad r = R; \\ \frac{\partial u_2}{\partial r} = v_2 = \frac{\partial T_2}{\partial r} &= 0, \quad r = 0. \end{aligned} \quad (17)$$

Restricting ourselves to the first term in expression (16), Eq. (17) need not be solved, since in this case it can be shown that

$$\langle q \rangle = - \left\langle \frac{\rho_0 c_p}{R} \int_0^R \left[r \frac{\partial (u_1 T_1)}{\partial x} + \frac{\partial (r v_1 T_1)}{\partial r} \right] dr \right\rangle.$$

Performing the integration, we obtain

$$\langle q \rangle = \frac{1}{8} \rho_0 c_0^2 |\bar{C}|^2 V \sqrt{2\nu\omega} \left\{ \left[\frac{2(1 - \operatorname{Pr}^{1/2})}{1 + \operatorname{Pr}} + \frac{\kappa + 1}{\operatorname{Pr}^{1/2}} - 1 \right] \cos 2(kx + \alpha_0) + \left[1 + \frac{\kappa - 1}{\operatorname{Pr}^{1/2}} \right] \operatorname{ch} 2\beta \right\}. \quad (18)$$

For small-amplitude oscillations the neglect of terms with ε^4 and higher terms is fully justified, and expression (18) can be considered as final. However, an estimate shows that for $\varepsilon \geq 0.1$ it is necessary to include the second term in (16). Averaging over time and integrating the fourth-order energy equation over cross section, we obtain

$$\begin{aligned} \lambda R \left\langle \frac{\partial T_4}{\partial r} \Big|_{r=R} \right\rangle &= c_p \rho_0 \left\langle \int_0^R r \left(u_2 \frac{\partial T_2}{\partial x} + v_2 \frac{\partial T_2}{\partial r} + u_3 \frac{\partial T_1}{\partial x} + u_1 \frac{\partial T_3}{\partial x} + \right. \right. \\ &+ \left. \left. v_3 \frac{\partial T_1}{\partial r} + v_1 \frac{\partial T_3}{\partial r} \right) dr \right\rangle + c_p \left\langle \int_0^R r \left(\rho_2 \frac{\partial T_2}{\partial t} + \rho_1 \frac{\partial T_3}{\partial t} + \rho_3 \frac{\partial T_1}{\partial t} \right) dr \right\rangle - \end{aligned} \quad (19)$$

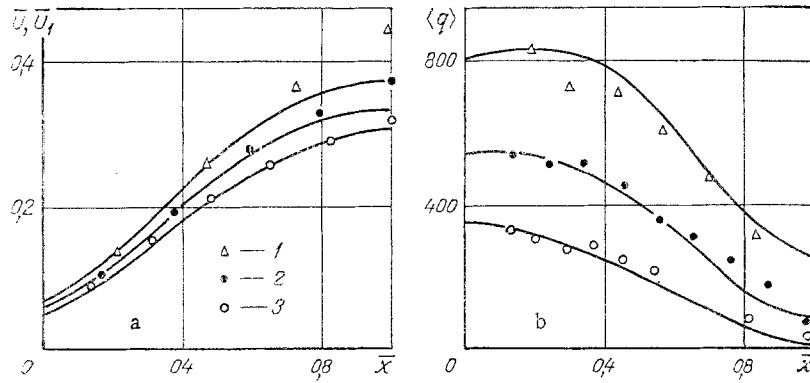


Fig. 1. Distribution of the dimensionless velocity fluctuation difference (points), dimensionless velocity fluctuation amplitude (curves) (a), and the thermal flux (points, experiment; curves, theory) (b) along the tube: 1) $L_0 = 3.485$ m; 2) 4.485 m; 3) 5.485 m.

$$-\mu \left\langle \int_0^R r \left[\left(\frac{\partial u_2}{\partial r} \right)^2 + 2 \frac{\partial u_1}{\partial r} \frac{\partial u_3}{\partial r} \right] dr \right\rangle - \left\langle \int_0^R r \left(u_2 \frac{\partial p_2}{\partial x} + u_1 \frac{\partial p_3}{\partial x} + u_3 \frac{\partial p_1}{\partial x} \right) dr \right\rangle.$$

The second- and third-order equations are very complicated. To take into account fourth-order effects we confine ourselves to the solution of the time-averaged Eq. (17). Putting $Pr = 1$ (so as to avoid awkward results), we obtain:

$$\begin{aligned} u_2 = & \frac{|C|^2}{8\rho_0^2 c_0^3} \left\{ \sin 2(kx + \alpha_0) \left[(2 + \kappa) \left(1 - 2 \frac{r^2}{R^2} \right) - 20 \frac{\delta}{R} \left(1 - \frac{r^2}{R^2} \right) - \right. \right. \\ & \left. \left. - (\kappa - 2) e^{-2\xi} + \kappa (e^{-(1+i)\xi} + e^{-(1-i)\xi}) - (\kappa - 4) i (e^{-(1+i)\xi} - e^{-(1-i)\xi}) \right] - \right. \\ & \left. - \text{sh } 2\beta \left[\kappa \left(1 - 2 \frac{r^2}{R^2} \right) - \kappa i (e^{-(1+i)\xi} - e^{-(1-i)\xi}) - \kappa e^{-2\xi} + \right. \right. \\ & \left. \left. + \kappa (e^{-(1+i)\xi} + e^{-(1-i)\xi}) \right] + 4\kappa \frac{\omega x}{c_0} \frac{\delta}{R} \left(1 - \frac{r^2}{R^2} \right) \text{ch } 2\beta \right\}, \\ v_2 = & \frac{\omega R |C|^2}{16\rho_0^2 c_0^4} \left\{ \cos 2(kx + \alpha_0) \left[(2\kappa + 4) \left(\frac{r^3}{R^3} - \frac{r}{R} \right) - \right. \right. \\ & \left. \left. - 20 \frac{\delta}{R} \left(\frac{r^3}{R^3} - 2 \frac{r}{R} \right) - (2\kappa^2 - 4) \frac{\delta}{R} e^{-2\xi} - (\kappa^2 + 8) \frac{\delta}{R} (e^{-(1+i)\xi} + \right. \right. \\ & \left. \left. + e^{-(1-i)\xi}) + (\kappa^2 + 2\kappa - 8) \frac{i\delta}{R} (e^{-(1+i)\xi} - e^{-(1-i)\xi}) \right] + \right. \\ & \left. + \text{ch } 2\beta \left[2\kappa \frac{\delta}{R} \left(\frac{r^3}{R^3} - 2 \frac{r}{R} \right) + 2 \frac{\delta}{R} (\kappa^2 - \kappa) e^{-2\xi} + \right. \right. \\ & \left. \left. + (2\kappa - \kappa^2) \frac{\delta}{R} (e^{-(1+i)\xi} + e^{-(1-i)\xi}) + \frac{i\kappa^2 \delta}{R} (e^{-(1+i)\xi} - e^{-(1-i)\xi}) \right] \right\}, \\ p_2 = & \frac{|C|^2}{4\rho_0 c_0^2} \cos 2(kx + \alpha_0), \end{aligned} \quad (20)$$

$$\begin{aligned} T_2 = & \frac{|C|^2}{8\rho_0^2 c_0^2 c_p} \left\{ \cos 2(kx + \alpha_0) [(\kappa + 1) + \kappa i (e^{-(1+i)\xi} - e^{-(1-i)\xi}) - \right. \\ & \left. - (\kappa + 1) (e^{-(1+i)\xi} + e^{-(1-i)\xi}) + (\kappa + 1) e^{-2\xi}] + \text{ch } 2\beta [(\kappa - 1) + \right. \\ & \left. + \kappa i (e^{-(1+i)\xi} - e^{-(1-i)\xi}) - (\kappa - 1) (e^{-(1+i)\xi} + e^{-(1-i)\xi}) + (\kappa - 1) e^{-2\xi}] \right\}, \end{aligned}$$

where u_2 , v_2 , p_2 , and T_2 are the averaged parts of the corresponding second-order quantities. Retaining in (19) only terms due to the interaction of given quantities, we have

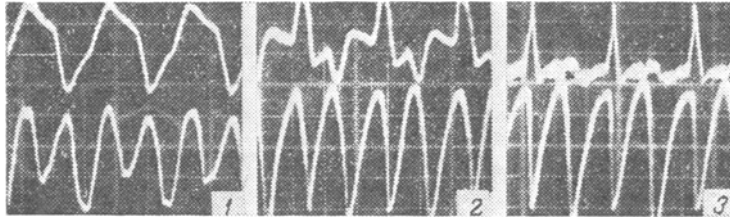


Fig. 2. Oscillograms of pressure (above) and velocity (below) at resonance in a tube of length $L_0 = 3.485$ m with different gain coefficients: 1) $\bar{x} = 0.211$; $\bar{P} = 0.72$; $\bar{U} = 0.14$; 2) $\bar{x} = 0.728$; $\bar{P} = 0.56$; $\bar{U} = 0.37$; 3) $\bar{x} = 0.987$; $\bar{P} = 0.27$; $\bar{U} = 0.45$.

$$-\dot{\lambda} \left\langle \frac{\partial T_u}{\partial r} \Big|_{r=R} \right\rangle = -\frac{c_{p0} \rho_0}{R} \left\langle \int_0^R r \left(u_2 \frac{\partial T_2}{\partial x} + v_2 \frac{\partial T_2}{\partial x} \right) dr \right\rangle + \frac{\mu}{R} \left\langle \int_0^R r \left(\frac{\partial u_2}{\partial r} \right)^2 dr \right\rangle + \frac{1}{R} \left\langle \int_0^R r u_2 \frac{\partial p_2}{\partial x} dr \right\rangle.$$

The final expression for $\langle q \rangle$ including fourth-order terms with $\kappa = 1.4$ is

$$\begin{aligned} \langle q \rangle = & \frac{1}{8} \rho_0 c_0^2 |\bar{C}|^2 \sqrt{2\nu\omega} \left\{ 1.47 \operatorname{ch} 2\beta + \frac{|\bar{C}|^2}{4} [7.07 + 0.389 \operatorname{ch}^2 2\beta + \right. \\ & + 1.366 \operatorname{sh}^2 2\beta] + 2 \cos 2(kx + \alpha_0) + \frac{|\bar{C}|^2}{4} [0.7 \sin 4(kx + \alpha_0) - \\ & - 4.54 \cos 4(kx + \alpha_0) + 4.74 \sin 2(kx + \alpha_0) \operatorname{sh} 2\beta - 12.09 \cos 2(kx + \alpha_0) \operatorname{ch} 2\beta - \\ & \left. - 1.4 \cos 2(kx + \alpha_0) \operatorname{sh} 2\beta + \frac{\omega x}{c_0} (3.36 \sin 2(kx + \alpha_0) - 2.8 \cos 2(kx + \alpha_0) \operatorname{ch} 2\beta) \right\}. \end{aligned} \quad (21)$$

The experimental part of this work includes the study of resonance oscillations in a semiopen tube and of thermal effects on its wall. Measurements of the distributions of velocity oscillation amplitudes along the tube and of resonance curves were carried out in an instrument described in detail in [6].

For the thermal measurements we prepared a probe, being a segment tube of length 0.1 m with flanges. To minimize heat losses in the axial direction of the probe to the bulk the tubes were connected through asbestos washers of thickness 0.01 m. The external surface of the probe was under conditions of free heat transfer with the surrounding medium with a constant heat-transfer coefficient, determined by the Kramers equation [7]. The wall temperature was measured by a thermocouple, and the temperature of the surrounding medium by a thermometer. The measurements showed that 20 min were sufficient to establish a stationary regime of heat transfer. Assuming that the temperature is uniform over the whole mass of the probe, one can write

$$m_{\text{inf}} c_p \frac{\partial T}{\partial t} = \langle q \rangle S_1 - \alpha^* S_2 (T - T_\infty). \quad (22)$$

Integrating (22) for initial condition $T = T_\infty$ at $t = 0$, and carrying out the limiting transition at $t = \infty$, we obtain $T_{\text{max}} = T_\infty + \langle q \rangle S_1 / \alpha^* S_2$, whence $\langle q \rangle = (T_{\text{max}} - T_\infty) (\alpha^* S_2 / S_1)$.

Figure 1a shows the distribution of experimentally measured dimensionless velocity fluctuation amplitude, calculated from expression (15), along the axis for three tube lengths. It follows from the figure that near the piston there is full agreement between theory and measurement. The deviation is maximum at the open end, but does not exceed 17% for a tube of length $L_0 = 3.485$ m. This is easily explained by considering the pressure (above) and velocity (below) fluctuation oscillograms, presented in Fig. 2, corresponding to different distances from the open end of the tube of length $L_0 = 3.485$ m. Near the piston the oscillations have a symmetric, nearly sinusoidal, shape. As the open end is approached the contribution of higher harmonics increases, and a shock is formed, while the acoustic approximation to the theory of resonance oscillations was obtained under the assumption of comparatively weak nonlinear oscillations. This fact explains the better agreement between results for longer tubes, though even for a tube with $L_0 = 5.485$ m the velocity amplitude reached 100 m/sec. The corresponding distributions of thermal flux are given in Fig. 1b. The theoretical results have the feature that in Eq. (21) $|\bar{C}|$ was replaced by the value of the velocity fluctuation amplitude at the open end. It is easily noted that $\langle q \rangle$ is maximum

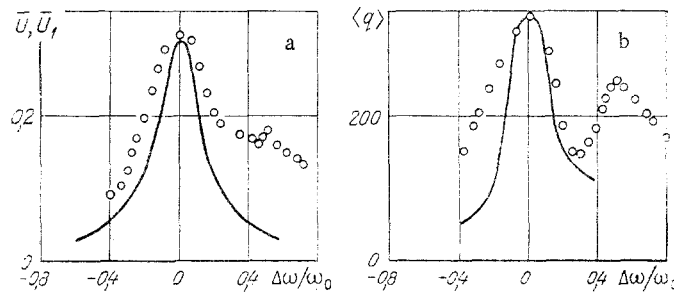


Fig. 3. Dependence of the dimensionless velocity fluctuation differences (points) and dimensionless velocity fluctuation amplitude (curves) at the open end (a) and of the thermal flux (points, experiment; curve, theory) (b) at $x = 0.125$ on $\Delta\omega/\omega_0$ in a tube of length $L_0 = 5.485$ m.

near the piston, i.e., where the velocity fluctuation amplitude is minimum. The thermal flux decreases upon getting away from the piston.

Figure 3 shows resonance curves of the dimensionless amplitude and difference of longitudinal velocity fluctuations (Fig. 3a) as well as $\langle q \rangle$ according to theory and experiment (Fig. 3b). It is seen that the theory describes the experimental results well near resonance. The deviation increases further away from the resonance frequency. At $\Delta\omega/\omega_0 = 0.5$ experiment shows a second nonlinear resonance of the thermal flux $\langle q \rangle$, though in Fig. 3a the second nonlinear resonance of velocity fluctuations is expressed quite weakly. This is easily explained by properties of the second nonlinear resonance [6].

Thus, the acoustic approximation to the theory of nonlinear oscillations, with the use of a nonlinear boundary condition at the open end, is quite suitable for a theoretical description of velocity fluctuation amplitudes reaching 150 m/sec. On this basis we succeeded in constructing a theory of thermoacoustic effects, describing satisfactorily experimental results with linear resonance.

NOTATION

L , tube length; R , radius; x , distance from the piston; r , radial distance from the tube axis; c_p and c_v , specific heats; μ , dynamic viscosity coefficient; λ , thermal conductivity; t , time; u and v , longitudinal and radial velocity components; p , pressure; ρ , gas density; T , gas temperature; R_g , universal gas constant; $\varepsilon = U_\infty/\omega L$, a small parameter; U_∞ , scale of velocity fluctuations; ω , angular frequency; c_0 , speed of sound; J_ν , first-kind Bessel function of the ν -th order; $\kappa = c_p/c_v$; A , B , C , and α , complex constants determined from the boundary conditions; $\nu = \mu/\rho$, coefficient of kinematic viscosity; $Pr = \nu/\alpha$, Prandtl number; $\alpha = \lambda/c_p\rho$, thermal diffusivity coefficient; $k = \omega/c_0$, wave number; l , piston displacement amplitude; Z , total impedance of the open end of the tube; Z_U , radiation impedance; X and Y , active and reactive parts of Z_U ; d , tube diameter; $|C|$, ψ , absolute value and phase of C ; α_0 and β , active and reactive parts of α ; $\langle q \rangle$, local time-averaged thermal flux to the tube wall; m_p , mass of the probe; c_p , specific heat of the probe material; S_1 and S_2 , areas of the inner and outer probe surfaces; T_∞ , temperature of the surrounding medium (ambient); α^* , heat-transfer coefficient to the surrounding medium; T_{\max} , maximum wall temperature that can be reached under given heat-transfer conditions; L_0 , real tube length, $\bar{x} = x/L$, dimensionless distance from the piston; $\bar{U}_1 = (u_1/c_0)_{\max}$, dimensionless velocity fluctuation amplitude at the axis; $\bar{U} = (u/c_0)_{\max}$, dimensionless velocity fluctuation difference; $\bar{P} = (P_2 - P_1)2P_0$, dimensionless pressure fluctuation difference; P_2 and P_1 , largest and smallest pressure values during an oscillation period; P_0 , atmospheric pressure; ω_0 , resonance frequency; $\Delta\omega = \omega - \omega_0$; $\delta = \sqrt{2\nu/\omega}$, width of the acoustic boundary layer; $| \cdot |$, a notation for amplitude; $\langle \cdot \rangle$ denotes time averaging.

LITERATURE CITED

1. P. Mercli and H. Thoman, "Thermoacoustic effects in a resonance tube," *J. Fluid Mech.*, **70**, 161-178 (1975).
2. R. G. Galiullin, V. B. Repin, and N. Kh. Khalitov, *Viscous Flow and Heat Exchange in a Sound Field* [in Russian], Kazan State Univ. (1978).

3. H. B. Dwight, Tables of Integrals and Other Mathematical Data, Macmillan, New York (1957).
4. J. H. M. Disselhorst and L. Van Wijngaarden, "Flow in the exit of open pipes during acoustic resonance," J. Fluid Mech., 99, 293-319 (1980).
5. V. B. Raushenbakh, Vibrational Heating [in Russian], Fizmatgiz, Moscow (1961).
6. R. G. Galiullin and G. G. Khalimov, "Study of nonlinear oscillations of a gas in open tubes," Inzh.-Fiz. Zh., 37, 1043-1050 (1979).
7. J. O. Hinze, Turbulence, McGraw-Hill, New York (1975).

THERMOPHYSICAL CHARACTERISTICS OF APROTONIC SOLVENTS AND ELECTROLYTES
BASED ON THEM

I. G. Gurevich, K. B. Gisina,
V. K. Shchitnikov, and B. I. Tumanov

UDC 536.223:541.135

Measured and computed values of the thermal conductivity and heat capacity of a number of organic solvents and electrolytes based on them are presented.

As we have already noted previously [1-2], there are no systematic data in the literature on the physicochemical properties of a comparatively new class of electrolytes (based on organic solvents), which are used in chemical power sources (CPS) with alkali metal anodes [3, 4]. This remark applies to an even greater extent to their thermophysical characteristics as well. At the same time, a knowledge of the latter is necessary for calculations of the thermal operational regimes of these sources.

We studied the temperature dependence of the thermal conductivity of such CPS solvents most widely used in practice: propylene carbonate (PC), γ -butyrolactone (γ -BL), tetrahydrofuran (THF), and their two-component mixtures. Lithium perchlorate (LiClO_4) was used as the ionogenic component of the electrolyte.

The procedure for cleaning and preparing the indicated solvents and electrolytes based on them for the experiment is described in detail in [1, 2].

In order to measure the thermal conductivity, we used the heated-probe method [5], using the apparatus developed at the ITMO AN BSSR [6]. The advantages of this method, which include the short time necessary for the tests (the duration of a single experiment does not exceed 60-90 sec), small overheating of the medium, and good contact between the medium and the sensor, were especially important in application to volatile liquids, such as the substances being studied.

The sensor-probe used in this work consisted of a coil 0.7 mm in diameter and length ~30 mm, made of a bifillar winding on a thin medical needle with diameter 0.5 mm of the heater (consisting of a manganese wire 0.1 mm in diameter with resistance 50-60 Ω) and a resistance thermometer (consisting of copper wire 0.05 mm in diameter with resistance of 3 Ω at 20°C); the probe was covered with a thin lacquer layer for electrical insulation and to increase the mechanical strength.* The dimensions of the probe and of the measuring cell (diameter 30 mm, height 85 mm) permitted us to reduce the intrinsic heat capacity of the former to a minimum and ensure that the boundary conditions of the corresponding heat conduction problem, on whose solution the method is based, are satisfied.

The so-called "relative" variant of the method, in which the thermal conductivity sought is determined by comparing the thermograms recorded on a potentiometer for a standard liquid and for the liquid being studied, is used on our apparatus.

*The probes had to be changed often due to the strong corrosive action of the solvents studied. Naturally, the new probe required calibration using a standard fluid.